Plasma membrane-associated proteins are clustered into islands attached to the cytoskeleton

Björn F. Lillemeier*, Janet R. Pfeiffer†, Zurab Surviladze†, Bridget S. Wilson†, and Mark M. Davis*‡

*Howard Hughes Medical Institute and Department of Microbiology and Immunology, Stanford University School of Medicine, Stanford, CA 94305; and †Department of Pathology and Cancer Research and Treatment Center, University of New Mexico, Albuquerque, NM 87131

Contributed by Mark M. Davis, October 16, 2006 (sent for review September 18, 2006)

Although much evidence suggests that the plasma membrane of eukaryotic cells is not homogenous, the precise architecture of this important structure has not been clear. Here we use transmission electron microscopy of plasma membrane sheets and specific probes to show that most or all plasma membrane-associated proteins are clustered in cholesterol-enriched domains (''islands'') that are separated by ''protein-free'' and cholesterol-low membrane. These islands are further divided into subregions, as shown by the localization of ''raft'' and ''non-raft'' markers to specific areas. Abundant actin staining and inhibitor studies show that these structures are connected to the cytoskeleton and at least partially depend on it for their formation and/or maintenance.

cholesterol | electron microscopy | microdomains | plasma membrane structure

In eukaryotes, the plasma membrane serves to segregate the cell from its environment and to serve as the principal interface for communication between cells. Thus, its structure and properties are likely to impact many biological processes. For many years, the ''fluid mosaic'' model of Singer and Nicolson (1) has shaped our view of the plasma membrane. In this model, proteins diffuse freely in a homogenous lipid environment. This model found support in the work of Frye and Edidin (2), who showed that surface proteins could diffuse throughout a plasma membrane. But subsequent results showed that protein diffusion is 5–50 times slower in the plasma membrane than in artificially reconstituted membranes or liposomes, suggesting that there are significant barriers to movement (3).

Another clue suggesting that the plasma membrane has a more complex architecture was the finding that it was not homogenous with regard to protein and lipid composition, leading to the ''lipid raft'' model of van Meer and Simons (4). This model suggests that rafts have a distinct lipid composition that requires cholesterol and renders them resistant to certain detergents (5, 6). The partitioning of specific proteins into these lipid rafts has been suggested to be important in many cases of cell surface receptor signaling.

Another type of analysis that has indicated that plasma membranes have distinct compartments is single-particle tracking, which has shown that a number of transmembrane proteins and lipids are restricted in their movement to ''confinement zones'' that vary in size from 30 to 700 nm, depending on the cell type, protein, or lipid (7, 8). Within these compartments, proteins can diffuse with coefficients similar to those in synthetic membranes or liposomes (7). These results and others have led to the ''picket-fence'' model, in which transmembrane proteins, like pickets, are anchored to and lined up along a fence of cytoskeletal proteins surrounding the confinement zones (9). Lastly, recent results using single-molecule imaging have shown that GFP-labeled molecules associated with the plasma membrane move within confined and, in at least some cases, nonoverlapping regions (10).

Recently, we became interested in using transmission electron microscopy of membrane sheets to try and approach the problem of plasma membrane structure (11). We adhered T cells and other cells to coated EM grids by a variety of procedures and ''ripped'' the adherent plasma membrane away from the rest of the cell. This procedure exposed the cytoplasmic face of the plasma membrane to antibodies and other specific markers. By using a variety of probes, we found that all membrane-associated proteins in the cells that we examined are clustered into what we refer to as ''protein islands'' that can be subdivided further into regions that can be labeled with a ''raft'' marker versus a ''non-raft'' marker. Furthermore, all of these protein-rich islands contain actin, which may provide a direct link to the cytoskeleton of the cell. We find the same results with other different cell types as well, suggesting that this type of organization is general and, thus, provides us with a new framework for understanding plasma membrane heterogeneity, function, and intercellular communication.

Results

Plasma Membrane Preparations from Activated and Nonactivated T Cells. Short-term cultures of lymph node cells from 5c.c7 T cell receptor (TCR) transgenic mice represent an abundant source of physiologically normal antigen-specific T cells. T cells were allowed to bind to EM grids coated either with poly-L-lysine (PLL) or the relevant peptide-MHC (I-E^K/MCC), plus costimulatory B7.1 molecules to mimic an antigen-presenting cell surface. T cells were bound to the PLL surfaces for 60 min at 37°C or alternatively preincubated with 50 μM PP2, a src kinase inhibitor that inhibits activation through the TCR and adhesion molecules, for 10 min at 37°C. Otherwise, T cells were activated for 3 min at 37°C on surfaces coated with I-E^K/MCC and B7.1.

The activation efficiency of the different surfaces with or without PP2 treatment was analyzed by using video microscopy to assess calcium signaling (12). Untreated T cells interacting with the PLL surfaces adhere and spread strongly. These surfaces also induce sporadic calcium fluxes of very low intensity. T cells adhere well to the activating surface, although spreading is significantly reduced compared with the PLL surface, suggesting that the latter involves Focal Adhesion Kinase. Calcium signaling by T cells on the activating surface is comparable in strength and profile with T cells activated by antigen-presenting cells (data not shown). PP2 treatment completely inhibits cell spreading and calcium signaling in cells interacting with any surface.

For the EM studies, T cells were bound to the coated grids as described above. A coverslip coated with PLL is attached to the

Author contributions: B.F.L., B.S.W., and M.M.D. designed research; B.F.L. performed research; B.F.L., J.R.P., Z.S., and B.S.W. contributed new reagents/analytic tools; B.F.L. analyzed data; and B.F.L. and M.M.D. wrote the paper.

The authors declare no conflict of interest.

Freely available online through the PNAS open access option.

Abbreviations: TCR, T cell receptor; PLL, poly-L-lysine.

‡To whom correspondence should be addressed at: Howard Hughes Medical Institute, Beckman Center, Room B221, 279 Campus Drive, Stanford, CA 94305. E-mail: mdavis@pmgm2.stanford.edu.

This article contains supporting information online at www.pnas.org/cgi/content/full/0609009103/DC1.

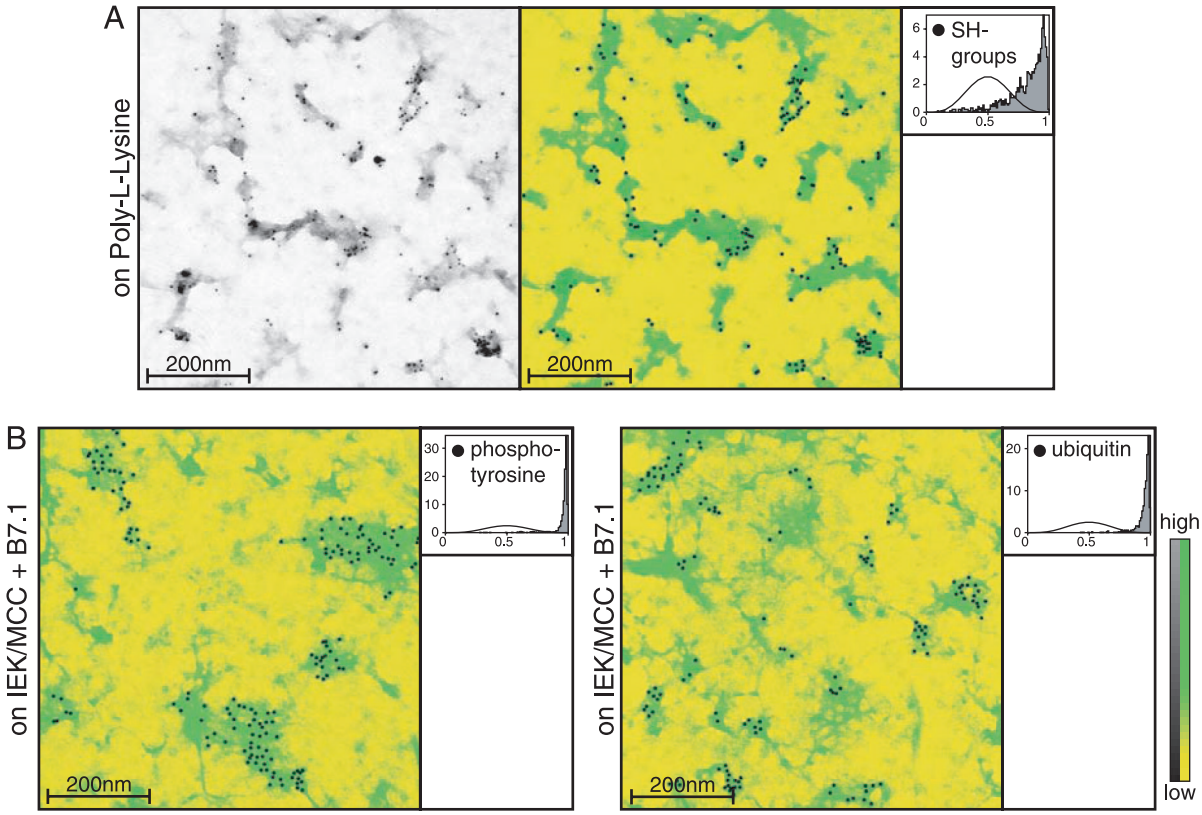

Fig. 1. Localization of membrane-associated proteins in T cells. (*A*) Membrane sheets from resting T cells (PLL surface after PP2 treatment) were biotinylated on SH groups. Biotinylated proteins were detected by using streptavidin-conjugated 5-nm gold particles. (*Left*) An unmodified image of a typical membrane sheet. (*Center*) The same image in pseudocolor with the gold particles shown in filled black circles. (*Right*) Graph showing clustering by Hopkins analysis. (*B*) Membrane sheets from activated T cells (I-E^k/MCC + B7.1 surface) were labeled with 5-nm gold particles for tyrosine phosphorylation (*Left*) and ubiquitinylation (*Right*). Images are shown in pseudocolor with the gold particles shown as filled black circles. Hopkins analyses for tyrosine phosphorylation (*Left*) and ubiquitinylation (*Right*) show significant clustering. The relationship between the EM stain and pseudocolor is shown in the false-color bar.

tops of the adhered cells. While slight pressure is applied to the coverslip using a rubber cork, excess liquid is removed by suction. The cells are then ripped by manual separation of the coverslip and the EM grid (11, 13–17), which leaves resting (on PLL) or activated (on I-E^K/MCC + B7.1) membranes bound to the grid [this procedure is illustrated in supporting information (SI) Fig. 5*A*]. The membranes are large (≈7–10 μm) sheets of plasma membrane with the cytoplasmic side exposed (SI Fig. 5*B*). After paraformaldehyde or paraformaldehyde/glutaraldehyde fixation, proteins were labeled with antibodies and other reagents bound to gold particles. The standard EM staining reagents osmium tetroxide, tannic acid, and uranyl acetate were applied sequentially to visualize membrane structures and add contrast. The quality of the fixation was examined by using fluorescent correlation spectroscopy of GFP-tagged raft and non-raft markers (described in *Visualizing Raft and Non-Raft Regions*) in "live" membrane sheets, demonstrating that membrane-attached proteins are rapidly immobilized upon addition of fixative (data not shown). The quality of the membrane sheets was also demonstrated by the preservation of cytoskeletal structures, clathrin coated pits, and vesicles (SI Fig. 5*B*). Examples of membrane sheets that were not used for analyses due to imperfections, like ruffles and holes, are shown in SI Fig. 5*C*.

All Membrane-Associated Proteins Are Clustered. In our analysis of both activated and resting T cell membranes, we saw a patchwork of dark and light staining regions, with the former occupying ≈20–50% of the plasma membrane depending on cell type and adhesion conditions (Fig. 1*A*). This pattern in T cells is very similar to that reported previously for mast cell, B cell, and fibroblast membranes (13–17). To better visualize these different regions, we used software that uniformly colors the EM images (Fig. 1*A*). All original images of membrane sheets are still on hand in either each figure or the supporting information. In our analyses and in those previously reported (13–17), antibodies directed at over a dozen cell surface and signaling proteins invariably labeled their targets within the darker contrast regions. These findings raised the possibility that all membrane-associated proteins would localize to these areas.

To test this hypothesis, we first analyzed membrane sheets from resting T cells. Proteins within the membrane sheets were biotinylated on sulfhydryl or carboxyl groups and labeled with streptavidin-gold (Fig. 1*A* and SI Fig. 6*A*). However, this labeling procedure did not label proteins that were exclusively on the extracellular side of the plasma membrane (e.g., glycosylphosphatidylinositol-anchored molecules) or had no available sulfhydryl or carboxyl groups in their cytosolic domains. In each case, the distribution of gold particles was analyzed for statistically relevant clustering by Hopkins analysis (18). In this analysis, a Gaussian distribution shows that the label was distributed randomly, whereas a shift to the right indicates clustering. The marked rightward shift in the Hopkins analysis and the localization of the gold label in these experiments indicates that in resting T cell membranes, proteins as a whole were clustered within the darker contrast regions (Fig. 1*A* and SI Fig. 6*A*, graphs) and that clustering was independent of the modification chemistry.

The results of these experiments are consistent with the

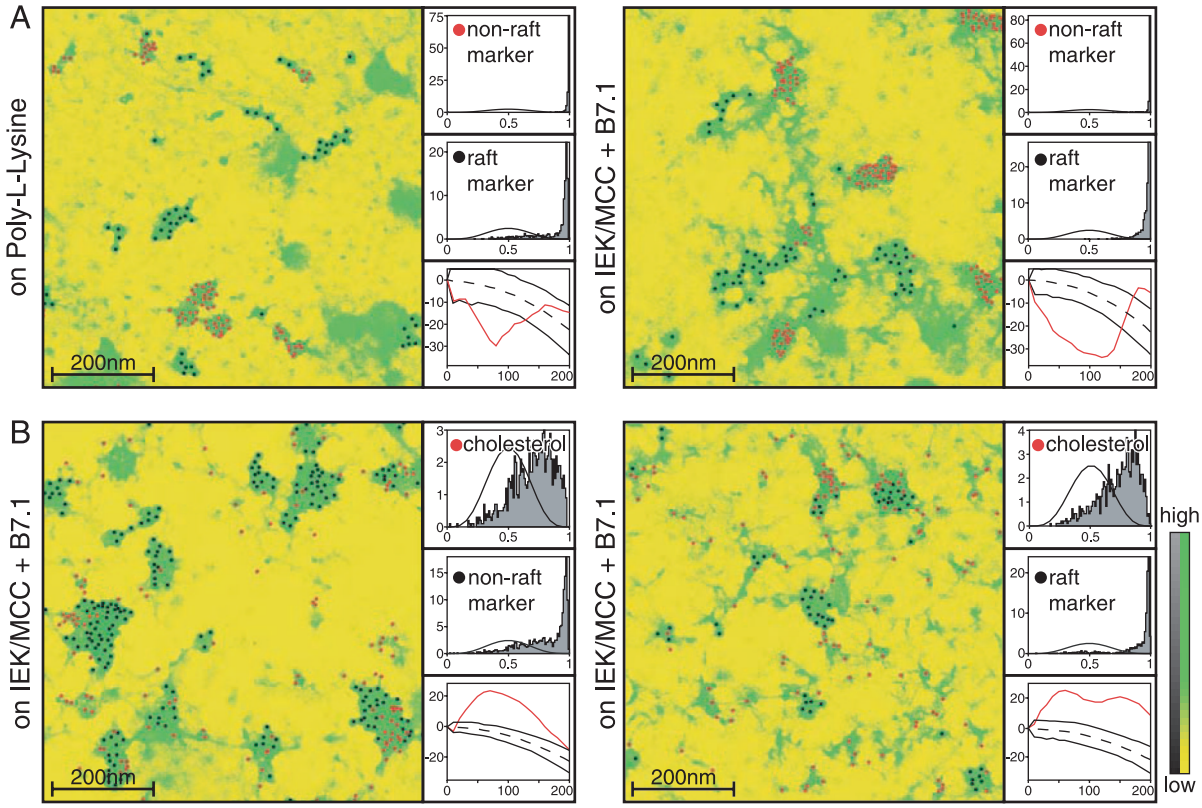

Fig. 2. Localization of raft and non-raft markers. (*A*) Membrane sheets from resting (*Left*) and activated (*Right*) T cells expressing tagged non-raft and raft markers, which are shown in filled red circles (5-nm gold particles) and filled black circles (10-nm gold particles), respectively. Hopkins analyses show clustering for the non-raft marker (top graphs) and raft marker (middle graphs). The Ripley's *K* analyses (bottom graphs) show repulsion or explicit separation. (*B*) Membrane sheets from activated T cells infected with either a non-raft (*Left*) or raft (*Right*) marker were stained for the expressed marker with specific antibodies (10-nm gold particles, filled black circles) and for cholesterol with perfringolysin *O* labeled with 5-nm gold particles (filled red circles). Hopkins analyses for cholesterol show slight clustering (top graphs), whereas the raft and non-raft markers are strongly clustered (middle graphs). Ripley's *K* analyses show colocalization for raft and non-raft markers with cholesterol (bottom graphs). The relationship between EM stain and pseudocolor is shown in the false-color bar.

hypothesis that the darkly staining regions in these membrane preparations contain most or all membrane-associated proteins. In >50 membrane sheets analyzed for protein localization by amino acid biotinylation, we did not detect any biotinylated proteins in low contrast areas. These results were repeated and confirmed in membrane sheets attached to PLL at 4°C and 37°C in the presence and absence of PP2 (data not shown).

The same biotinylation patterns were observed in membrane sheets from MDCK (dog kidney), RBL-2H3 (rat basophil), and CHO (Chinese hamster ovary) cells adhering to PLL-coated EM grids (SI Fig. 7). Consequently, this finding that membrane-associated proteins are clustered within the darker staining regions is most likely true for most, if not all, eukaryotic cell types.

We wanted to investigate this phenomenon in activated T cells. However, biotinylation of SH groups in membrane sheets is possible only on EM grids coated with PLL, because the SH groups within the immobilized ligands on an activating surface cause strong background labeling. Therefore, we stained membrane sheets from activated T cells with antibodies specific for posttranslational modifications. These results show that all detectable tyrosine phosphorylation, ubiquitinylation, and symmetrical or asymmetrical dimethylation localized exclusively to the dark areas (Fig. 1*B* and SI Fig. 6*B*). Hopkins analyses for all of these stains show strong clustering (Fig. 1*B* and SI Fig. 6*B*, graphs). We also assessed the same protein modifications in membrane sheets from nonactivated T cells on PLL (with or without PP2 treatment) and obtained similar results (data not shown). As expected, tyrosine phosphorylation was strongly reduced in nonactivated T cells and undetectable after PP2 treatment.

All of the above results together show that all proteins associated with the plasma membrane were clustered in regions of higher contrast, which we propose to call protein islands.

Visualizing Raft and Non-Raft Regions. The existence of lipid rafts in plasma membranes has been an area of considerable controversy. To label lipid rafts, we used the N-terminal 10 aa of the tyrosine kinase lck (containing a N-terminal myristoylation site and two S-palmitoylation sites) plus five additional lysine residues and either a tandem HA- or Myc-tag as a raft marker (19, 20). This marker was transformed into a non-raft marker with a "myristate plus basic" signal by mutating its S-palmitoylation sites from cysteine to alanine (20). Both constructs were expressed and localized in membrane sheets from resting and activated T cells (Fig. 2*A* and SI Fig. 8*A*). All experiments were repeated with inverted gold sizes and tags. Each tag was detected with antibodies from different species. Noninfected T cells did not show any label with the antibodies specific to the tags. Together, the two markers occupied 45–60% of the protein islands, and neither was detectable in the lighter staining regions. As shown by Hopkins analysis, each marker was highly clustered with respect to itself (Fig. 2*A* and SI Fig. 8*A*, top and middle graphs). Colocalization was analyzed by using bivariate Ripley's *K* statistic (21, 22). The bivariate Ripley's *K* analysis is shown by a plot of $L(t) - t$ (y axis) versus distance in nanometers (x axis). $L(t) - t$ values represent the number of differently sized neighbors to any gold particle within a certain distance. The

black dotted line shows the theoretical values of $L(t) - t$ for two randomly colocalizing gold labels with the same staining intensities as in the image. A data curve (represented by a red line) is based on the actual localization of gold particles in an image and has to lie above the 99% confidence envelope (represented by black lines) to show statistically significant attraction or association of two differently sized gold labels or below it to show their repulsion or explicit separation. The two markers are clearly separated when analyzed in this way (Fig. 2*A* and SI Fig. 8*A*, bottom graphs). Interestingly, we find that in the activated membrane sheets the raft and non-raft clusters are more aggregated, with contacts between raft and non-raft regions becoming more frequent. Therefore, the common border increases in length (Fig. 2A and Fig. 8A), indicating functional influences on the protein island morphology. The small number of raft markers in non-raft areas is consistent with previously published results and presumably reflects continuous depalmytoylation (19, 23). These results show that both raft and non-raft proteins are clustered and occupy distinct areas within the protein islands.

Another characteristic of lipid rafts is thought to be their enrichment for cholesterol and their loss of "detergent resistance" after depletion of cholesterol with methyl-β-cyclodextrin (6). We detected cholesterol in the inner leaflet of membrane sheets from resting and activated T cells with monomeric perfringolysin-*O* conjugated to 5-nm colloidal gold (24). Cholesterol distribution was specifically compared with that of the raft or non-raft markers described above. Remarkably, cholesterol is present throughout the protein islands, where it colocalizes with both raft and non-raft markers visually and by Ripley's *K* statistics (Fig. 2*B* and SI Fig. 8*B*, bottom graphs). In contrast, cholesterol is dramatically reduced in the protein-free areas. Hopkins analyses show that the distribution of cholesterol is non-random (Fig. 2*B* and SI Fig. 8*B*, top graphs) but less ordered than either marker (Fig. 2*B* and SI Fig. 8*B*, middle graphs). We also treated T cells with the cholesterol-depleting reagent methyl-β-cyclodextrin and could no longer detect the perfringolysin-*O* gold labeling (data not shown). However, depletion of cholesterol has no significant influence on the localization or clustering of the raft and non-raft markers in the membrane sheets of resting or activated T cells, suggesting that cholesterol is not required for localization of membrane-associated proteins to the protein islands (data not shown), although it may well be for functional properties.

Actin Anchors the Protein Islands. Numerous studies have shown that the cytoskeleton plays an important role in membrane compartmentalization. Therefore, membrane sheets from resting and activated T cells were stained with antibodies to either actin (all six isoforms) or β-tubulin. Actin is detected abundantly in most protein islands and is excluded from the light staining areas (Fig. 3*A* and SI Fig. 9*A*). This finding is in contrast to β-tubulin, which can be detected in only a subset (SI Fig. 9*A*). In additional experiments, both actin and β-tubulin colocalize with the raft and the non-raft markers (SI Fig. 9*A*).

The heavy actin staining that we see associated with these islands suggests that actin polymerization might play an important role in the structure of these entities. A technical problem with using actin-depolymerizing reagents is that they prevent cells from adhering to surfaces (data not shown). Thus, we surface-biotinylated amine groups on T cells and then incubated them with either cytochalasin D or with the more potent actin-depolymerizing agents latrunculin A or B for 90 min at 37°C. Cells were then attached to EM grids coated with streptavidin for an additional 60 min at 37°C in the presence of the drugs. A coverslip coated with streptavidin was applied to the tops of the cells bound to the EM grid, followed by ripping and paraformaldehyde fixation. EM grids were further treated as described above. Untreated and drug-treated T cells do not spread as much on this surface, and the density of the protein islands was significantly increased compared with the previous ripping techniques (Fig. 3*B* and SI Fig. 9*B*). Remarkably, all drug treatments led to a dramatic reduction in the density of the protein islands, with latrunculin A having the greatest effect

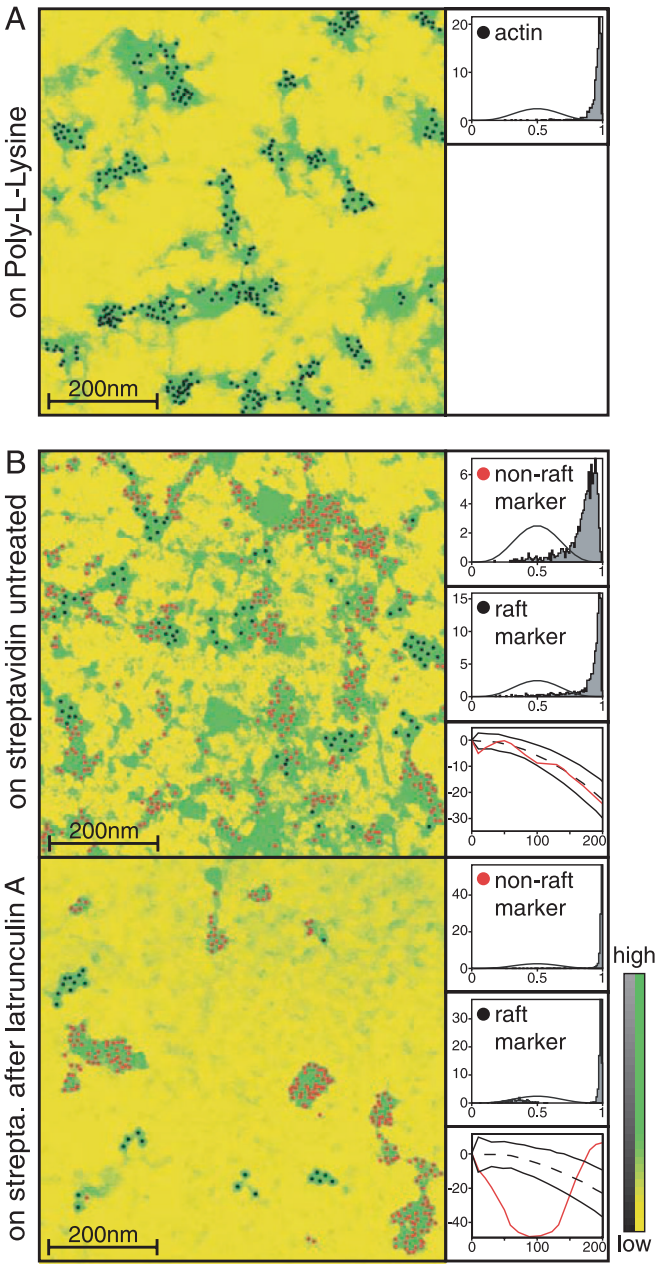

Fig. 3. Cytoskeletal association of protein islands. (*A*) Membrane sheets from resting T cells were stained for actin (all six isoforms) with 5-nm gold particles (filled black circles). Hopkins analysis shows clustering (graph). (*B*) T cells were surface-biotinylated on NH_2 groups and cultured for 90 min with (*Upper*) or without (*Lower*) 20 μM latrunculin A. T cells were adhered to streptavidin-coated EM grids for an additional 60 min in the continued absence or presence of the drug and ripped by using a streptavidin-coated coverslip. In both cases, Hopkins analysis shows clustering for raft and non-raft markers in the untreated and latrunculin A-treated cells (top and middle graphs, respectively). Because of the high density of protein islands in the membrane sheets from untreated T cells, no explicit separation can be detected with Ripley's *K* function (bottom graphs). However, the markers still show separation in the latrunculin A-treated cells (bottom graphs). An obvious reduction in the number of protein islands after latrunculin A treatment is visible. The relationship between EM stain and pseudocolor is shown in the false-color bar.

CELL BIOLOGY

(Fig. 3*B* and SI Fig. 9*B*). The raft and non-raft markers were still clustered and localized to the dark staining regions (Fig. 3*B* and SI Fig. 9*B*, top and middle graphs). Raft and non-raft regions were distinct according to Ripley's *K* statistic and comparable in size to protein islands in untreated cells (Fig. 3*B* and SI Fig. 9*B*, bottom graphs). Interestingly, the protein islands in the membrane sheets from drug-treated cells still contained actin (SI Fig. 9*C*). This result is most likely due to short actin filaments or G-actin monomers.

In contrast to these results, disrupting microtubule polymerization with nocodazole under a variety conditions had no obvious effect on rafts, non-rafts, or the protein islands in general (data not shown).

Discussion

Our results using membrane sheets derived from short-term cultured T cells and three other cell lines indicate that the plasma membrane is divided into compartments that contain membrane-associated proteins surrounded by protein-free regions. The latter is supported by atomic force microscopy studies of membrane sheets, showing similar sized regions with the thickness of a lipid bilayer (25). (These studies also show that most membrane sheets generated with this method have a continuous lipid bilayer.) The protein islands described here have diameters of ≈30–300 nm, which are very similar to the sizes reported for membrane confinement zones analyzed by using single-particle tracking. Structures of this size are just at or below the limits of fluorescence detection, which explains why they have not been seen previously. We are able to subdivide these protein islands into raft and non-raft regions by using lck-derived raft and non-raft markers. However, not all protein-containing regions were labeled with these two probes. This result and the localization of other raft and non-raft resident proteins suggest a greater complexity to the protein islands than just these designations.

We find that protein islands are enriched for cholesterol, with very little in the protein-free regions, indicating that cholesterol enrichment is not a unique feature of only detergent-resistant membranes or raft structures but is a feature of all protein-containing compartments. Cholesterol could, of course, be used differently in raft regions versus non-raft regions.

The heavy actin staining of these protein islands and their reduced density in membrane sheets after actin depolymerization suggests a close linkage to the cytoskeleton, although given the rapidity with which proteins diffuse in the plasma membrane, it is unlikely that this connection is very rigid. That actin might have a major role in the structure of these regions was indicated in previous single-molecule studies by an increase in the size of confinement zones and therefore a reduction of "hop-diffusion" rates (molecule movement from one confinement zone to another) and a slight increase in macroscopic diffusion rates after the depolymerization of actin (e.g., refs. 3, 7, and 26). However, several studies failed to see an effect of these agents on the movement of membrane-associated molecules (e.g., refs. 26 and 27).

The pattern of high- and low-contrast staining regions using this approach has previously been seen in a wide variety of other cell types (e.g., mast cells, B cells, fibroblasts, ovarian cancer cells, and lymphocytes) (13–17). Because membrane proteins tagged by antibody probes invariably localize to areas of high contrast, the protein island structures that we describe here are likely to be a general characteristic of all or most cell types.

The results described here were obtained by using paraformaldehyde- or paraformaldehyde/glutaraldehyde-fixed membranes. Therefore, one potential artifact is that the observed clustering is due to cross-linking of proteins during fixation. However, the molecules cluster in distinctly non-random ways, such as in the differential clustering of raft and non-raft markers on activating surfaces versus nonactivating surfaces, despite the fact that they cannot interact with the surfaces themselves (Fig. 2*A*). Furthermore, published data found by using this same protocol has shown that Fc Receptor I on mast cells clusters independently of the adaptor protein LAT (linker for activation of T cells) and associated molecules and that they then move together (but do not interdigitate) upon activation (14). We have very similar results in the T cell system described here showing that TCR/CD3 complexes clustering independent from LAT and that they move together in an activated cell (unpublished data).

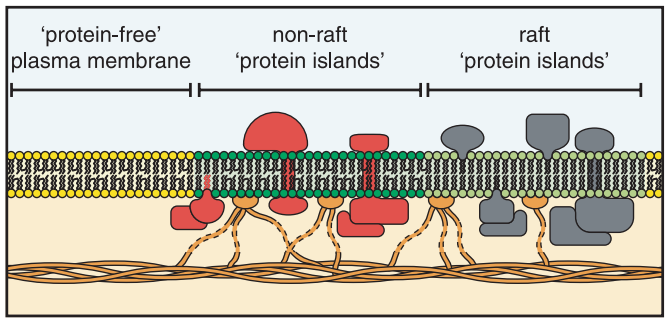

Fig. 4. The protein island model. In this model all membrane-associated proteins are clustered in protein islands (green lipids) that are surrounded by a sea of protein-free membrane (yellow lipids). The islands can be subdivided into raft and non-raft islands, which is also illustrated by their lipid composition (bright-green and dark-green lipids, respectively) and protein contents (gray and red proteins, respectively). Molecules move with high diffusion rates within the islands, and the islands themselves can move with significant restrictions in the membrane. The protein islands are connected to the cytoskeleton (orange), most likely by actin because it plays a crucial role in island formation and/or maintenance. We propose that theses islands can exchange proteins and lipids by hop diffusion when in physical contact.

Other possible artifacts due to the interaction of cells with the surface of the EM grid were excluded by using three different adhesion methods (immobilized ligands, PLL, and streptavidin) with T cells. On all three surfaces, very similar or identical protein islands were detected.

The data presented here suggest a different model of plasma membrane organization. The original fluid mosaic model of Singer and Nicolson (1) has already been modified over the years into several different models of plasma membrane compartmentalization, driven by evidence suggesting the existence of lipid rafts (4–6) and confinement zones, the detection of hop diffusion (7), and the influence of actin on compartmentalization (7, 26) as well as recent single-molecule studies (10). Additionally, T cell activation induces the formation of TCR-containing microclusters, which can fuse to form larger clusters (28). The latter supports our results showing aggregation of raft and non-raft islands (Fig. 2*A* and SI Fig. 8*A*) and TCR/CD3 complexes and LAT clusters in T cells adhered to an activating surface (unpublished data). These phenomena and our results can all be encompassed into the protein island model (Fig. 4), in which proteins localize to "proteinphilic" membrane compartments, probably because of protein–protein interaction and/or their affinity for certain lipids. These protein islands are separated and surrounded by a "sea" of protein-free membrane and are linked to the actin cytoskeleton. These actin anchors and the larger actin polymers in the cortical cytoskeleton most likely play a key role in protein island formation and/or maintenance, as suggested by the inhibitor studies described here. The dynamics and flexibility of the actin cytoskeleton would allow these compartments to be mobile with a certain degree of restriction. Raft regions occupy distinct regions within these protein islands, and previous work has shown that they are uniquely sensitive to cholesterol depletion, suggesting that they have a distinctive structure and function. There may be multiple types of raft

regions, as some have suggested, or it may be that different raft resident proteins can localize to different regions on a cell surface by segregating within protein islands (16). There may be protein species that do not congregate in these islands, given that our analyses do not include glycosylphosphatidylinositol-linked proteins or molecules with no available sulfhydryl or carboxyl groups in their cytosolic domains.

Our findings have implications for many cellular events involving the plasma membrane. Activation thresholds, segregation, and transduction of signaling pathways at the plasma membrane are all likely to be influenced by the compartmentalization of membrane-associated proteins into protein islands. Protein islands may also play a role in cell–cell communication, membrane trafficking, and membrane fusion. Therefore, although many aspects of the protein islands are unknown at this time, we hope that the results described here will be a useful framework for further investigation and thinking about the structure and function of the plasma membrane.

Materials and Methods

T Cell Culture. T cells were isolated from lymph nodes of 5c.c7 TCR-transgenic mice and stimulated with MCC peptide with or without retroviral infection with the Phoenix system (29). Cells were maintained in RPMI medium 1640 plus 10% FCS. IL-2 at 30 units/ml was added to the cells after 24 h in culture. Cells were harvested on day 6 or 7.

Preparation of Plasma Membrane Sheets and Gold Labeling. Formvar- and carbon-coated nickel EM grids were coated with PLL as described (13) or sequentially with biotinylated PLL, streptavidin, and biotinylated I-E^K/MCC and B7.1. Cells were allowed to attach to the differently coated grids. The grids were rinsed, placed on an acetate disk, and covered with PLL- or streptavidin-coated coverslips. Pressure was applied to the coverslip by bearing down with a cork. The coverslips were lifted, leaving the lower cell surface adherent to the coated EM grid. Membranes were fixed immediately after the ripping procedure. Membrane sheets were labeled with the appropriate detection reagents and postfixed followed by sequential OsO_4, tannic acid, and uranyl acetate staining as described (13). Grids were air-dried and examined by transmission electron microscopy.

EM Data Analysis. Negatives of membrane sheets were digitized and machine-based colored. The positions of the gold particles are indicated by circles (Figs. 1–3) according to their positions determined during the mapping of gold particles for the statistical analysis. Mapping gold particle distribution and statistical analyses were performed as previously described (21, 22).

For additional details, see *SI Materials and Methods*.

We thank Dr. Art Johnson (Texas A&M University, College Station, TX) for the monomeric perfringolysin-*O* construct and John Perrino and Jon Mulholland (Stanford University) for support. Spatial statistics methods were developed by Drs. S. Steinberg, J. Zhang, K. Leiderman, and D. Roberts at the University of New Mexico/Sandia National Laboratories Center for Spatiotemporal Modeling under National Institutes of Health Grant P20 GM66283. This work was supported by National Institutes of Health Grants AI225511 (to M.M.D.) and AI051575 (to B.S.W.) and a grant from the Howard Hughes Medical Institute (to M.M.D.). B.F.L. was supported by a postdoctoral fellowship from the Human Frontier Science Program Organization.

1. Singer SJ, Nicolson GL (1972) *Science* 175:720–731.
2. Frye LD, Edidin M (1970) *J Cell Sci* 7:319–335.
3. Sheetz MP, Schindler M, Koppel DE (1980) *Nature* 285:510–511.
4. van Meer G, Simons K (1982) *EMBO J* 1:847–852.
5. Yu J, Fischman DA, Steck TL (1973) *J Supramol Struct* 1:233–248.
6. Ilangumaran S, Hoessli DC (1998) *Biochem J* 335:433–440.
7. Sako Y, Kusumi A (1994) *J Cell Biol* 125:1251–1264.
8. Simson R, Sheets ED, Jacobson K (1995) *Biophys J* 69:989–993.
9. Kusumi A, Ike H, Nakada C, Murase K, Fujiwara T (2005) *Semin Immunol* 17:3–21.
10. Douglass AD, Vale RD (2005) *Cell* 121:937–950.
11. Sanan DA, Anderson RG (1991) *J Histochem Cytochem* 39:1017–1024.
12. Wulfing C, Sjaastad MD, Davis MM (1998) *Proc Natl Acad Sci USA* 95:6302–6307.
13. Wilson BS, Pfeiffer JR, Oliver JM (2000) *J Cell Biol* 149:1131–1142.
14. Wilson BS, Pfeiffer JR, Surviladze Z, Gaudet EA, Oliver JM (2001) *J Cell Biol* 154:645–658.
15. Prior IA, Muncke C, Parton RG, Hancock JF (2003) *J Cell Biol* 160:165–170.
16. Wilson BS, Steinberg SL, Liederman K, Pfeiffer JR, Surviladze Z, Zhang J, Samelson LE, Yang LH, Kotula PG, Oliver JM (2004) *Mol Biol Cell* 15:2580–2592.
17. Kim JH, Cramer L, Mueller H, Wilson B, Vilen BJ (2005) *J Immunol* 175:147–154.
18. Jain AJ, Dubes RC (1988) *Algorithms for Clustering Data* (Prentice Hall, Englewood Cliffs, NJ).
19. Zlatkine P, Mehul B, Magee AI (1997) *J Cell Sci* 110:673–679.
20. van't Hof W, Resh MD (2000) *Methods Enzymol* 327:317–330.
21. Ripley BD (1977) *J R Stat Soc B* 39:172–212.
22. Zhang J, Leiderman K, Pfeiffer JR, Wilson BS, Oliver JM, Steinberg SL (2006) *Micron* 37:14–34.
23. Ike H, Kosugi A, Kato A, Iino R, Hirano H, Fujiwara T, Ritchie K, Kusumi A (2003) *ChemPhysChem* 4:620–626.
24. Ramachandran R, Tweten RK, Johnson AE (2005) *Proc Natl Acad Sci USA* 102:7139–7144.
25. Frankel DJ, Pfeiffer JR, Surviladze Z, Johnson AE, Oliver JM, Wilson BS, Burns AR (2006) *Biophys J* 90:2404–2413.
26. Murase K, Fujiwara T, Umemura Y, Suzuki K, Iino R, Yamashita H, Saito M, Murakoshi H, Ritchie K, Kusumi A (2004) *Biophys J* 86:4075–4093.
27. Vrljic M, Nishimura SY, Brasselet S, Moerner WE, McConnell HM (2002) *Biophys J* 83:2681–2692.
28. Varma R, Campi G, Yokosuka T, Saito T, Dustin ML (2006) *Immunity* 25:117–127.
29. Pear WS, Nolan GP, Scott ML, Baltimore D (1993) *Proc Natl Acad Sci USA* 90:8392–8396.